Electrical, optical and theoretical characterization of doped and undoped calamitic liquid crystal: (s)-5-octyloxy-2-[[[4-(2-methyl butoxy) phenyl] imino] methyl] phenol

M. SERIN[a,*], F. KURUOGLU[a], M. MOGULKOC[a], M. CALISKAN[a], Y. YALCIN-GURKAN[b], O. YASA-SAHIN[c], D. SAKAR[c], B. BILGIN-ERAN[c]
[a]*Department of Physics, Yildiz Technical University, Istanbul 34210, Turkey*
[b]*Namik Kemal University, Department of Chemistry, Değirmenaltı Campus, 59030 Tekirdağ, Turkey*
[c]*Department of Chemistry, Yildiz Technical University, Istanbul 34210, Turkey*

The electrical conductivities of undoped and doped calamitic liquid crystalline compound, (S)-5-octyloxy-2-[[[4-(2-methylbutoxy) phenyl] imino] methyl] phenol (OMPIMP) with tetrabutylammonium tetrafluoroborate as dopant were determined as a function of temperature. Optical studies of undoped and doped OMPIMP thin films were also carried out using spectrophotometer. Optical band gaps of doped and undoped OMPIMP thin films were determined through absorption spectra using Tauc plot. The frontier orbital energies; E_{HOMO}, E_{LUMO} and the band gap energies were calculated from the DFT calculations which were carried out by the hybrid B3LYP functional.

(Received January 24, 2014; accepted May 15, 2014)

Keywords: Calamitic liquid crystals, Electrical conductivity, Phase transition temperature, Optical band gap energy, Density functional theory

1. Introduction

The term liquid crystal (LC) is used to describe an aggregation state whose properties are intermediate between a crystalline solid and an amorphous liquid. The field of liquid crystals covers a vast range of synthetic and organic materials generally composed of calamitic molecules with orientational, but not longrange positional order [1-4].

In recent years, LC materials have received huge attention due to their optical properties and applications both in our daily life (cell phones, lap top displays, digital watches, calculators, etc.) and scientific optical applications such as tunable waveguides, digital holography, optical processors, diffraction gratings, optical tweezers etc. [5]. Liquid crystals composed of calamatic molecules are still widely investigated because of using application in optoelectronic devices, prerequisites for the development of mobile communication and information processing systems. An essential issue in developing semiconductor devices for photovoltaics and thermoelectrics is to design materials with appropriate band gaps plus the proper positioning of dopant levels relative to the bands [6-9].

Modern density functional theory (DFT) provides an extremely valuable tool for predicting structures and energetics of new materials for both finite and periodic systems. Some correlations have been found between dipole moments and polarizabilities with the calculated ones through the use of semiempirical quantum chemical methods. There are also some structure–property relationships reported in the literature [10-17]. But the results obtained through the use of these equations deviate from the experimental values due to the parameterization in semiempirical methods. Therefore, more sophisticated methods, either *ab initio* or DFT methods are needed to improve them. Due to the limitations of today's computer power, these calculations can be performed using very simple, rigid, rod models. However, quantum chemical calculations are able to give the equilibrium geometry, electronic structure, electron density and charge distribution, dipole moment and the energy differences between various molecular conformations.

In this study, we report the electrical conductivity (as a function of temperature) and optical absorption of undoped and doped calamitic salicylaldimine and DFT calculation of undoped one at room temperature.

2. Experimental

The calamitic salicylaldimine compound, (S)-5-octyloxy-2-[[[4-(2- methylbutoxy) phenyl] imino]methyl]phenol, OMPIMP was synthesized (Fig. 1). The preparation procedure and spectroscopic data for OMPIMP salicylaldimine were given in us in Ref. [18].

Electrical characterizations were carried out on the base of dc conductivity–temperature measurements together with its variation with temperature. Undoped and doped samples under study were prepared by solving and mixing of OMPIMP and dopant in chloroform with a given concentration and deposited on thoroughly cleaned ITO glass substrate using analytical pipettes in air by solvent casting method. Tetra-n-butylammonium tetrafluoroborate (BF_4) as dopant was used to prepare doped samples at a ratio of 25 %. Aluminum electrode was prepared to form a sandwich - type specimen, according to Ref [19].

Dark conductivity of the produced films were measured as a function of temperature using a Janis liquid nitrogen vacuum cryostat, having a thermocouple in good thermal contact with the sample. Samples were placed on top of a copper plate. Temperature was recorded and controlled by Lakeshore Temperature Controller 331. The temperature dependence of conductivity was measured as the temperature being increased at a constant ratio as 3^oC min^{-1}.

Dark conductivity measurements were accomplished using a programmable Keitley 6517A digital electrometer / voltage source interfaced to a computer. The change in the conductivity of the sample was experimentally measured under the constant electrical field with a voltage, 50V. The measurements were carried out in $l0^{-5}$ Torr vacuum and the dark. The electrical conductivity of the polymer was measured in Al/OMPIMP/ITO structure over the temperature range of 303-383 K by heating and 383-303 K by cooling.

UV–Visible absorption spectra were recorded using a Perkin Elmer Lambda 2S UV-VIS Spectrophotometer. The absorption edge was analyzed to obtain the optical band gap of undoped and doped OMPIMP.

3. Results and discussion

3.1. Phase Transitions of OMPIMP

The chemical structure, transition temperatures, corresponding enthalpy values and mesophase type observed for the OMPIMP is summarized in Table 1. The details of preparation procedures, all spectroscopic data and liquid crystalline properties for the OMPIMP were given in Ref [18].

According to the results, OMPIMP exhibits liquid crystalline properties and shows thermotropic enantiotropic mesophase. The investigations by optical polarizing microscopy show that it exhibits smectic C* (SmC*) mesophase.

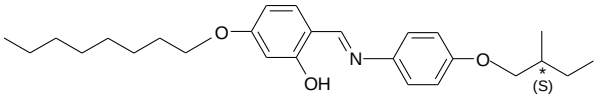

Fig. 1. Chemical structure of compound OMPIMP.

Table 1. Phase transition temperatures[a] T (°C) and transition enthalpies[a] ΔH (kJ mol^{-1}) of compound OMPIMP. Cr: crystalline, SmC: chiral smectic, Iso: isotropic phase.*

Compound	T/°C (ΔH/kJ mol^{-1})
OMPIMP	Cr 31.2 (24.8) SmC* 84.3 (11.4) Iso

[a]Perkin-Elmer DSC-7; heating rates 10 K min^{-1} for the melting and clearing process; the enthalpies are in parentheses.

3.2. Electrical characterization of undoped and doped OMPIMP

Electrical characterization of the films was realized on the base of dc conductivity-temperature measurements for the films undoped and BF_4 doped with 25 % ratio. The temperature dependence of the electrical conductivity was measured in the temperature range of 303-383 K. Electrical conductivity can be described by the exponential dependence on temperature:

$$\sigma_D = \sigma_0 \exp(-E_a / kT) \quad (1)$$

where σ_D is the dark conductivity, E_a is the activation energy, and σ_0 the preexponential factor [20,21]. The conductivity is obtained by measuring the current flowing through a piece of the material and using the sample dimensions to calculate σ from the equation.

The electrical conductivities of undoped and doped OMPIMP were measured from room temperature to 120^oC by heating and then cooling (Figs. 2 and 3). The phase transitions were determined from the Arrhenius plot of conductivity of Al / OMPIMP / ITO and Al / doped OMPIMP / ITO structures from heating and cooling data. The obtained results were summarized in Table 2.

The electrical conductivity of doped OMPIMP thin films, indicating a transition from "*Cr* phase" to "*Iso* phase", increased as seven orders of the magnitude with increasing temperature while the electrical conductivity of undoped OMPIMP thin films increased as four orders of the magnitude. The electrical conductivity of doped OMPIMP thin films decreased as three orders of the magnitude while the electrical conductivity of undoped OMPIMP decreased as five orders of the magnitude with cooling.

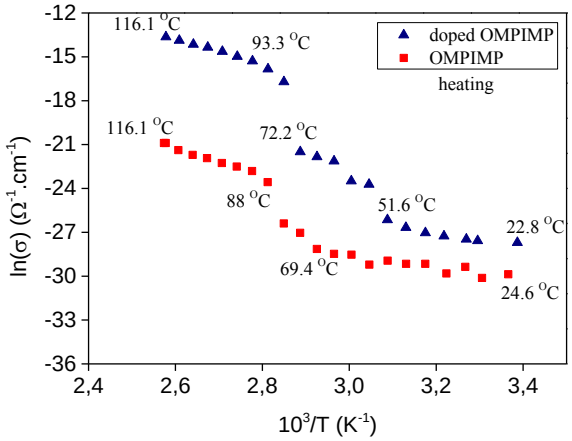

Fig. 2. Arrhenius plot of conductivity for Al/OMPIMP/ITO and Al/doped OMPIMP/ITO structure by heating.

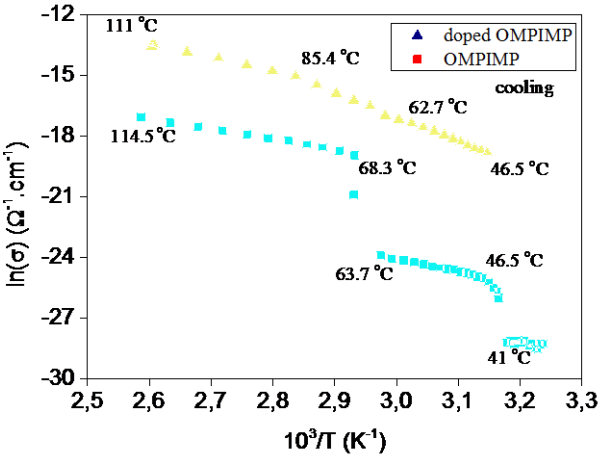

Fig. 3. Arrhenius plot of conductivity for Al/OMPIMP/ITO and Al/doped OMPIMP/ITO structure by cooling.

Table 2. The electrical conductivities of undoped and doped OMPIMP by heating and cooling and phase transitions.

σ_D of undoped OMPIMP	
Heating (°C); (phase)	Cooling (°C); (phase)
1.06×10^{-13} (25); Cr	4×10^{-8} (114.5); Iso
6×10^{-12} (69.4); SmC*	8×10^{-10} (68.3); SmC*
1.25×10^{-10} (88.0); Iso	4×10^{-11} (63.7); SmC*
1.0×10^{-9} (116.1); Iso	3×10^{-13} (35); Cr

σ_D of doped OMPIMP	
Heating (°C); (phase)	Cooling (°C); (phase)
9×10^{-14} (25); Cr	1.3×10^{-6} (111); Iso
4×10^{-12} (51.6); SmC*	3×10^{-7} (85.4); Iso
5×10^{-10} (74.2); SmC*	4×10^{-8} (62.6) SmC*
2×10^{-7} (93); Iso	7×10^{-9} (46.5); Cr

3.3. Optical characterization of doped and undoped OMPIMP

The band gaps of undoped and doped OMPIMP from optical absorption spectrums of undoped and doped OMPIMP were calculated using the Tauc equation [22] given by following equation for direct transition:

$$(\alpha h\nu) = A(h\nu - E_g)^m \qquad (2)$$

where m is a constant of 1/2 for allowed transitions and A is a constant.

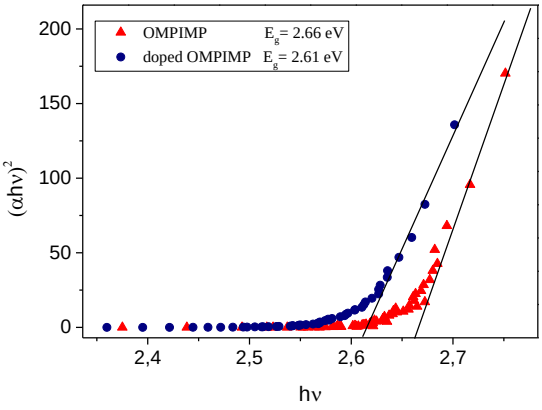

Fig. 4. Tauc plots of undoped and doped OMPIMP as a function of the photon energy.

The energy band gap of undoped and doped OMPIMP are found by extrapolating the linear part of $(\alpha h\nu)^2$ (as ordinate) against the photon energy $(h\nu)$ (as absisca) as shown in Fig. 4. The intercept of this line (extrapolation of Tauc plot to $\alpha^2 = 0$) determines the optical band gap energy. The energy band gaps of undoped and doped OMPIMP were determined as 2.66 eV and 2.61 eV, respectively.

3.4 Computational set-up

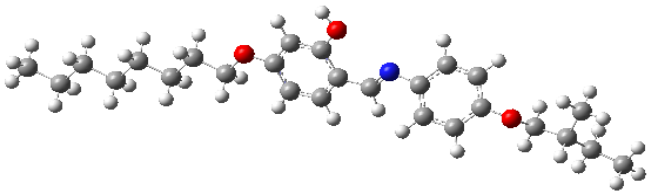

Fig. 5. Optimized geometry of OMPIMP (Grey, carbon; white, hydrogen; red, oxygen; blue, nitrogen).

The band gap (difference between the ionization potential and the electron affinity) is obtained from the difference in the orbital energies of the LUMO (conduction band minimum) and the HOMO (valence

band maximum) is obtained from a single calculation. The calculation was carried out using the Density Functional Theory (DFT) method within the GAUSSIAN 03 package [23] due to the fact that it takes electron correlation into account.

The DFT calculations were performed by the hybrid B3LYP functional which combines Hartree-Fock (HF) and Becke exchange terms with the Lee-Yang-Parr correlation functional. The cluster geometry was frozen throughout all the calculations, but the structure of OMPIMP complex was optimized in Fig. 5.

The geometric parameters, the frontier orbital energies; E_{HOMO}, E_{LUMO} and the band gap energy, E_g were calculated and given in Fig. 6.

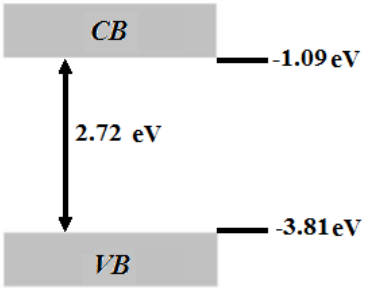

Fig. 6. Electronic structures of (S)-5-octyloxy-2-[[[4-(2-methyl butoxy)phenyl]imino]methyl]phenol with DFT /B3LYP method.

HOMO and LUMO energy value of OMPIMP were calculated from DFT calculation as -3.81 eV, -1.09 eV, respectively. The difference between them is the band gap of OMPIMP to be found as 2.72 eV. The value 2.72 eV is in agreement with the value obtained via Tauc relation for OMPIMP from absorption measurements.

4. Conclusions

Undoped and doped samples under study were prepared by solving and mixing of synthesized calamitic salicylaldimine compound, (S)-5-octyloxy-2-[[[4-(2-methylbutoxy) phenyl] imino]methyl]phenol, OMPIMP and dopant in chloroform with a given concentration and deposited onto ITO glass substrate. Tetra-n-butylammonium tetrafluoroborate (BF4) as dopant was used to prepare doped samples at a ratio of 25%.

The investigations realized by optical polarizing microscopy show that undoped OMPIMP exhibit liquid crystalline properties at room temperature and phase transition temperatures were determined for *Cr:crystalline*, *SmC*: chiral smectic and Iso: isotropic phase* as the temperature increased and decreased. From electrical conductivity measurements, we determined the same transition temperatures for the undoped and also doped OMPIMP.

The electrical conductivities of undoped and doped OMPIMP were determined as a function of temperature. The electrical conductivity of doped OMPIMP thin film was increased as seven orders of the magnitude and decreased as three orders of the magnitude while the electrical conductivity of undoped OMPIMP thin film was increased as four orders of the magnitude and decreased as five orders of the magnitude with increasing and decreasing temperature, respectively.

Optical absorption studies of undoped and doped OMPIMP thin films were also carried out using spectrophotometer to determine optical band gaps of doped and undoped OMPIMP thin films using Tauc plot. The frontier orbital energies; E_{HOMO}, E_{LUMO} and the band gap energies; E_g were calculated from the DFT calculations which were carried out by the hybrid B3LYP functional.

The energy band gaps of undoped and doped OMPIMP were determined as 2.66 eV and 2.61 eV, respectively, by absorption measurements and seen that this value was in agreement with the value determined as 2.72eV for undoped OMPIMP by Density Functional Theory (DFT) method.

Acknowledgement

This research has been supported by Yildiz Technical University Scientific Research Projects Coordination (Project Numbers: 2012-01-01-KAP05 and 2012-01-02-KAP08).

References

[1] C. Tschierske, J. Mater. Chem. **11,** 2647 (2001).
[2] M. G. Tamba, B. Kosata, K. Pelz, S. Diele, G.Pelzl, Z. Vakhovskaya, H. Kresse, W. Weissflog, Soft Matter. **2**, 60 (2006).
[3] N. Yilmaz Canli, S. Gunes, A. Pivrikas, A. Fuchbauer, D. Sinwel, N. S. Sarıciftci, O. Yasa, B. Bilgin-Eran, Sol. Energ. Mat. Sol. Cells. **94**, 1089 (2010).
[4] S. A. Jewell, Liq. Cryst. **38**, 1699 (2011).
[5] A. Iwana, H. Janeczek, A. Hreniak, M. Palewicz, D. Pociecha, Liq. Cryst. **37 (8),** 1021 (2010).
[6] B. Donnio, B. Heinrich, H. Allouchi, J. Kain, S. Diele, D. Guillon, D.W. Bruce, J. Am. Chem. Soc. **126**, 15258 (2004).
[7] C. Y. Liu, J. L. Chen, K. T. Liu, Anal. Chim. Acta. **384**, 51 (1999).
[8] A. Iwan, Mol. Crys. Liq. Cryst. **528,** 156 (2010).
[9] N. Yilmaz-Canli, A. Nesrullajev, O. Yasa, B. Bilgin-Eran, J. Optoelectron. Adv. Mater. Symp. **1**(3), 577 (2009).
[10] M. Villanueva-Garcia, R.N. Gutierrez-Parra, A. Martinez-Richa, J. Robles, J. Mol. Struct. (THEOCHEM). **727**, 63 (2005).
[11] P. D. Ojha, V. G. K. M. Pisipati, Liq. Cryst. **29**(7), 979 (2002).
[12] D. Demus, T. Inukai, Liq. Cryst. **26**(9), 1257 (1999).
[13] B. A. Belyaev, N. A. Drokin, V. F. Shabanov, V. A.

Baranova, Phys. Solid State. **46**(3), 574 (2004).
[14] S. J. Clark, C. J. Adam, G. J. Ackland, J. White, J. Crain, Liq. Cryst. **22**(4), 469 (1997).
[15] F. Eikelschulte, S. Yakovenko, D. Paschek, A. Geiger, Liq. Cryst. **27**(9), 1137 (2000).
[16] P. R. Richardson, S. P. Bates, J. Crain, A. C. Jones, Liq. Cryst. **27**(6), 845 (2000).
[17] C. J. Adams, S. J. Clark, G. J. Ackland, J. Crain, Phys. Rev. **55**(5), 5641 (1997).
[18] N. Yilmaz Canli, S. Günes, A. Pivrikas, A. Fuchsbauer, D. Sinwel, N. S. Sariciftci, Ö. Yasa, B. Bilgin-Eran, Sol. Energ. Mat. Sol. Cells. **94**(6), 1089 (2010).
[19] F. Sesigür, D. Şakar, O. Yasa-Sahin, F. Kuruoglu, F. Cakar, M. Mogulkoc, M. Calıskan, O. Cankurtaran, M. Serin, B. Bılgın- Eran, Optoelectron. Adv. Mater.-Rapid Comm. **5**(5), 572 (2011).
[20] Electrical Properties of Polymers, Ed. by D.A. Seanor, Academic Press, (1982).
[21] M. Serin, D. Sakar, O. Cankurtaran, F. Karaman, J. Optoelectron. Adv. Mater. **8,** 1308 (2006).
[22] J. Tauc, Amorphous & Liquid Semiconductors, New York: Plenum, 159 (1974).
[23] M. J. Frisch, G. W. Trucks, H. B. Schlegel, G. E. Scuseria, M. A. Robb, J. R. Cheeseman, J. A. Montgomery Jr., T. Vreven, K. N. Kudin, J. C. Burant, J. M. Millam, S. S. Iyengar, J. Tomasi, V. Barone, B. Mennucci, M. Cossi, G. Scalmani, N. Rega, G. A. Petersson, H. Nakatsuji, M. Hada, M. Ehara, K. Toyota, R. Fukuda, J. Hasegawa, M. Ishida, T. Nakajima, Y. Honda, O. Kitao, H. Nakai, M. Klene, X. Li, J. E. Knox, H. P. Hratchian, J. B. Cross, C. Adamo, J. Jaramillo, R. Gomperts, R. E. Stratmann, O. Yazyev, A. J. Austin, R. Cammi, C. Pomelli, J. W. Ochterski, P. Y. Ayala, K. Morokuma, G. A. Voth, P. Salvador, J. J. Dannenberg, V. G. Zakrzewski, S. Dapprich, A. D. Daniels, M. C. Strain, O. Farkas, D. K. Malick, A. D. Rabuck, K. Raghavachari, J. B. Foresman, J. V. Ortiz, Q. Cui, A. G. Baboul, S. Clifford, J. Cioslowski, B. B. Stefanov, G. Liu, A. Liashenko, P. Piskorz, I. Komaromi, R. L. Martin, D. J. Fox, T. Keith, M.A. Al-Laham, C. Y. Peng, A. Nanayakkara, M. Challacombe, P. M. W. Gill, B. Johnson, W. Chen, M.W. Wong, C. Gonzalez, J. A. Pople, Gaussian 03, Revision B.04, Gaussian, Inc., Pittsburgh, PA, 2003.

*Corresponding author: merihserin@gmail.com, serin@yildiz.edu.tr